Smart geometrical approach to intercalate a highly absorbing and quite resistive electron donor layer in ternary organic photovoltaic cells

L. Cattin, C. Cabanetos, A. El Mahlali, L. Arzel, M. Morsli, P. Blanchard, J.C. Bernède

Smart geometrical approach to intercalate a highly absorbing and quite resistive electron donor layer in ternary organic photovoltaic cells.

L. Cattin[1], C. Cabanetos[2], A. El Mahlali[1], L. Arzel[1], M. Morsli[3], P. Blanchard[2], J. C. Bernède[2*]

1- Institut des Matériaux Jean Rouxel (IMN), CNRS, UMR 6502, Université de Nantes, 2 rue de la Houssinière, BP 32229, 44322 Nantes cedex 3, France
2- MOLTECH-Anjou, UMR 6200, UNIV Angers, CNRS, 2 bd Lavoisier, 49045 ANGERS Cedex, France.
2*- MOLTECH-Anjou, CNRS, UMR 6200, Université de Nantes, 2 rue de la Houssinière, BP 92208, Nantes, F-44000 France.
3- Département de Physique, Université de Nantes, 2 rue de la Houssinière, BP 32229, 44322 Nantes cedex 3, France

Summary:
Ternary organic photovoltaic cells (OPVs) have been shown to be a promising approach to increase cells efficiency through broadening of their absorption range. Often, ternary cells are based on a blend of two donors and one acceptor, the efficiency of planar ternary heterojunction being limited by the resistance of the three stacked layers. Here, we show that by depositing the intercalated layer through a grid we are able to decrease significantly the series resistance of the device, while the use of two donors allows improving the short circuit current and the efficiency of the organic photovoltaic cells. Electrical, optical and morphological studies show the ternary cell behaves like parallel OPVs. The first donor layer consists in an AlPcCl film, the acceptor layer is a C_{60} film while the central layer consists in a laboratory made molecule called MD2. If the MD2 layer absorbs strongly the light and permits to the both types of carrier to diffuse, its carriers mobility is small. Therefore, the discontinuities, due to the grid, of the MD2 intercalated layer allow improving the cells efficiency over-passing the corresponding binary cells performances.

Keywords: Ternary organic photovoltaic cells; Band scheme matching; Charge carrier mobility; Optical properties; Surface roughness.
***Corresponding author:** J. C. Bernède ; E-mail address: jean-christian.bernede@univ-nantes.fr,

1. Introduction

In front of global warming it is necessary to develop renewable energies such as photovoltaic energy. Among the photovoltaic energy technologies, that based on the use of organic materials is promised to a bright future in the field of buildings due to the fact that organic photovoltaic solar cells (OPVs) are flexible, lightweight and semi-transparent [1]. In recent months, significant efficiency improvement of bulk-heterojunction organic photovoltaic solar cells (BHJ-OPVs) were achieved through the use of small band gap polymers coupled with new fullerene free electron acceptors [2, 3]. While it is desirable to improve cell performance, other parameters are also very important such as the yield of chemical synthesis, its simplicity and its reproducibility. For instance, the replacement of polymer by molecular materials presents some advantages such as the reproducibility of the results due to their inherent mono-dispersity, well-defined structure and simple purification [4].

In the same spirit, molecular materials offer the possibility to prepare efficient planar heterojunction (PHJ) OPVs by vacuum deposition [5]. The use of thermal evaporation under vacuum permits possible management of the film morphology through the deposition rate [6] and the nature of the substrate [7]. Also, the deposition by sublimation allows improving the purity of the organic materials, leading to high reproducibility of device fabrication [5, 8, 9].

Classical PHJ-OPVs consist of a stack of layers, the photoactive heart consisting of two organic layers, one electron donor (ED) layer and one electron acceptor (EA) layer. This organic active part is sandwiched between two electrodes, a transparent electrode and a reflective metallic electrode. In order to improve the carrier collection efficiency, hole and electron extracting layers are inserted between the electrodes and the organic active layer.

Whatever the OPV configuration is, BHJ or PHJ, the ultimate achievable efficiency is limited by the narrow absorption spectra of organic materials. It is possible to broaden the absorption range through the tandem OPVs approach which has granted high efficiency [10, 11]. Efficiency as high as 15% was achieved with tandem cells, one of them being deposited under vacuum while the second one was deposited using wet technique [12]. However, the short circuit current density (Jsc) of such device corresponds to that of the diode giving the smaller Jsc [13]. So, it is required to control carefully the fabrication receipt, which makes it a difficult structure to implement in practical OPVs. To overpass this difficulty, device architectures employing three molecular species in a cascade energy alignment can be used [13-18]. Efficiencies higher than 13.7% using ternary polymer solar cells based on bulk heterojunction were published [19]. On the other hand, good performances were obtained using simple ternary PHJs, *i.e.* OPVs with three organic layers, as demonstrated in different

examples [20-28]. Among these publications, very promising results were obtained [25]. Moreover, with industrial perspectives in mind, it is necessary to compare general performances of OPVs, *i.e.* reproducibility, ease and yield in chemical synthesis of new molecules and not only the OPVs efficiency alone. Actually, efficiency is only one of the criteria for the commercialization of OPVs. Other important criteria are the ease to synthesize molecules and their stability. Among these simply scalable and cost effective molecular material for OPV, a family of arylamine based push-pull derivatives has been developed in the MOLTECH-Anjou Laboratory [29]. It appears that the molecule MD2, presented in Figure 1, has emerged as a central material in this compound family [4, 30]. It can be synthesized in only two steps [31] and, when it is co-evaporated with C_{60} in multi-layers BHJ-OPVs it allows achieving 4% of efficiency [32]. Nevertheless, its modest hole mobility (μ_h = 1.0 10^{-5} $cm^2V^{-1}s^{-1}$) limits its charge transport properties. Therefore, many small push-pull analogues to MD2 were developed to overcome this limitation and as shown by Cabanetos et al. [29] promising results were achieved. Another way of investigation consists in introducing MD2 in ternary OPV using a smart geometrical approach that makes it possible to use its potential in OPVs while limiting the negative effect of its high resistivity. This is what we have tried to do in this work. After selecting a commercial electron donor whose band structure is compatible with that of MD2, we optimized the geometry of the stacked layers so as to limit the series resistance of the cell. Due to its light absorption complementarity with MD2, the dye elected was AlPcCl (aluminum phthalocyanine chloride), while as EA we used fullerene C_{60}.

We named “ternary OPVs” those based on the three layer structures AlPcCl/MD2/C_{60}, while those using a simple couple, AlPcCl/C_{60}, MD2/C_{60} or AlPcCl/MD2, were called binary structures (Supporting information S1a,b).

As shown by the band scheme of figure 2, the AlPcCl/MD2/C_{60} stacked layers exhibit a cascade band scheme, with sufficient HOMO and LUMO offsets for efficient exciton dissociation. Also, the open circuit voltage value being limited by the energy difference between the HOMO of the outmost donor and the LUMO of the EA, the maximum expected value is quite large, *i.e.* 1.25 V. In order to broaden the light absorption, by introducing MD2 between AlPcCl and C_{60} in the ternary structure, without increasing too significantly its series resistance, we have deposited the MD2 layer through a grid.

In these conditions, the ternary structure behaves as if it is constituted of independent parallel structures: anode/AlPcCl/C_{60}/cathode and anode/AlPcCl/MD2/C_{60}/cathode structures. Such

parallel structure avoids too large series resistance increase, thanks to the parallel-linkage mechanism of these OPVs, which improves the efficiency of the OPV.

2. Experimental

2.1 Organic molecules

The chemical structures of the organic molecules used during this work are shown in Figure 1. Organic molecules, AlPcCl, C_{60}, and BCP, and also CuI, MoO_3, Al were provided by CODEX-International (France) while 2-((5-(4(diphenylamino)phenyl)thiophen-2-yl)methylene)malononitrile (MD2) was synthesized as previously reported [30].

2.2 Organic photovoltaic cells deposition process and characterization

The preparation of the ITO coated glass substrates and experimental conditions used for the OPV realisation were previously presented [33]. Therefore they are briefly described in the supporting information S2 and S3. The schematic representations of the OPVs are shown in S1a and S1b. The characterization techniques used during this study are presented in the supporting information S3. Here we simply list them in order to introduce their acronyms for future use: space charge limited current (SCLC) method to estimate carrier mobility, current density-tension (J-V) characteristics, External Quantum Efficiency (EQE), Optical transmission measurements, Atomic Force Microscopy (AFM) and Scanning Electron Microscopy (SEM) studies.

As said above, hole and electron extracting layers are desirable to improve the power conversion efficiency (η) of the OPVs. As hole extracting layer (HEL), a double layer MoO_3/CuI was inserted between the ITO anode and ED. We have already shown that this HEL leads to optimized efficiencies [34, 35]. On the other hand, an exciton blocking layer (EBL) such as a bathocuproine (BCP) layer, was inserted between the EA and the Al cathode [36]. This layer is also acts as an Electron Transport Layer. More specifically, in the case of PHJ, it was called “exciton blocking layer (EBL)” because it blocks exciton transport towards the cathode. This avoids exciton quenching at the contact organic / cathode and protects the electron acceptor layer during the cathode deposition by evaporation [36-38].

The structures used were as follow:

Glass / ITO (100 nm) / MoO_3 (3 nm) / CuI (1.5 nm) / organic active layers / BCP (9 nm)/ Al (120 nm), the different configurations of the organic active layers are presented in the next paragraph.

3. Experimental results

3.1 Electrical (SCLC, J-V and EQE) and optical studies.

In a ternary PHJ-OPV the central layer must be ambipolar in order to allow the diffusion of charge carriers of both types, holes and electrons.

It was already shown that some organic molecules leading to ambipolar materials can be used as intercalated layer in ternary structures [39, 40]. Here, as we propose to use MD2 as central layer because its band structure is well adapted to this use (Figure 2). Its hole mobility being known, we first measured the electron mobility of MD2, to check its ambipolar character and hence to ensure its possible use as central layer in ternary structures. In these ternary PHJ-OPVs, AlPcCl was the donor and C_{60} was the acceptor. According to the protocol described in S3.1, the measurement of the electron mobility, μe, was performed through the use of electron only structures: ITO/Ca/MD2/LiF/Al. We have also checked the hole mobility, μh, using hole only devices: ITO/MoO_3/MD2/MoO_3/Al. The measured hole mobility, $\mu h = 1\ 10^{-5}$ cm^2/Vs, corresponds to the expected value [29, 32]. The electron mobility is $\mu e = 1.6\text{-}3.3\ 10^{-6}$ cm^2/Vs. As we will see, these relatively limited carrier mobilities will lead us to look for a smart geometrical strucure in order to be able to use MD2 effectively as an intermediary layer in a ternary PHJ-OPV.

After this preliminary study, we have measured the J-V characteristics of AlPcCl/MD2/C_{60} ternary PHJ-OPVs. In parallel to the study of these ternary OPVs, we studied binary OPVs from all possible combinations deduced from the ternary structure in order to verify if the multiple interfaces within the ternary structure are all active or not. So, we fabricated a set of PHJ- OPVs based on AlPcCl/C_{60}, MD2/C_{60} and AlPcCl/MD2 couples as control devices.

The optimization of the thickness of the organic active layers is reported in the supporting information S4, while the more significant results are reported in Table 1 and Figure 3. In Table 1, the main parameters of each the different OPVs categories are presented. The Figure 3a shows the J-V characteristics of the different binary OPVs, while the Figure 3b is dedicated to the optimization of the MD2 intercalated layer.

About the binary OPVs, the best result is obtained with AlPcCl, while the worst result is due to the couple AlPcCl/MD2. The results obtained with the couples AlPcCl/C_{60} [41] and MD2/C_{60} [29] are similar to those already published. The quite limited efficiency value

obtained with the couple AlPcCl/MD2 is probably due to the poor quality of its interface and to the small electron mobility of MD2. It can be seen that, when a classical, *i.e.,* a continuous MD2 film is intercalated between the AlPcCl and C_{60} films in a ternary structure, the efficiencies achieved are lower than those of the binary structures. This is due to a large decrease of the fill factor and a limited value of Jsc. These limitations are related to the increase of the series resistance. When the MD2 layer is thick of 15 nm, the J-V characteristics are S-shaped which can be attributed to the very high series resistance value (Table 1). For thinner MD2 layer the series resistance decreases and Jsc increases significantly. Nevertheless FF is still limited and, the performance increase, which can be obtained through the thickness decrease of the MD2 layer**,** allows matching the performances of the binary OPVs only for a zero MD2 layer thickness. As evidenced by the series resistance value, this is due to the fact that the carrier mobilites in MD2 are limited. Therefore, it was necessary to find a geometrical configuration that permits to overcome this bottleneck. We have already shown that by using as a first electron donor layer, a layer whose morphology allows the ternary structure to behave as it was two diodes in parallel, significant efficiency can be obtained [42]. We have used this phenomenon but by controlling it. To do this, we have used a grid to known geometry, and we have evaporated the MD2 layer through this grid, in order to obtain a discontinuous MD2 layer. As shown in table 1 and Figure 3b, such approach leads to performances which overpass those of the binary structures. The grid was made from heavy-duty 250 µm diameter steel wire spaced of 375 µm, giving 375 x 375 µm square holes (Figure 4a). It means that, roughly 40% of the AlPcCl under layer was covered by MD2 (Figure 4b).

As shown by the profile of Figure 5, the MD2 layer deposited through the grid resulted in cobbles whose thickness corresponds well to the value measured using the quartz monitor, in the present case 7 nm, while their width is 375 µm which corresponds to the expected value.

The schematized morphology of the OPVs obtained when the MD2 layer of the ternary PHJ is deposited through the grid is shown in Figure 6. The arrows indicate the band scheme of the structures corresponding to the both kind of structures encountered in such devices, either the ternary AlPcCl/MD2/C_{60} ternary OPV or the AlPcCl/C_{60} binary OPV. Such an alternating structure makes it possible to significantly decrease the series resistance (Table 1), while it allows benefiting from the current contribution due to the absorption of light by MD2. The EQE study permits to confirm this result (Figure 7a). In order to compare the shape of the EQE spectra with that of light absorption we have measured the optical density of the different films, alone and when they are staked. The absorption spectra of the different layers

used and that of their stack are represented in Figure 7b. The total absorption of the stacked layers corresponds to the sum of the absorption of the different stacked layers.

At first glance, depending of the ternary structure, it can be seen that the EQE spectra follow, more or less, the shape of the absorption spectrum of the stacked layers. The EQE signal between 575 and 815 nm corresponds to the main absorption band of AlPcCl, even if some MD2 contribution from 575 to 700 nm must not be ruled out. The central part of the EQE spectrum, between 400 and 600 nm must be attributed to MD2. Finally, the EQE signal in the small wavelength range can be attributed to both materials and, also, to C_{60}. This attribution of the various contributions to the EQE spectrum allows us to discuss the influence of the thickness and morphology of the MD2 layer. When the MD2 thickness is 15 nm, the series resistance of the diode is very high and the OPV efficiency is small, the same applies to the EQE signal. The AlPcCl being far from the acceptor, its contribution is very small. If that of MD2 is clearly visible, it is also relatively small, which is in good agreement with the small Jsc measured in these OPVs. When the MD2 layer thickness decreases, the series resistance of the ternary OPV decreases and its efficiency increases. The increase of the current is clearly due to a large increase of both contributions, AlPcCl and MD2. Nevertheless, the contribution of AlPcCl is still quite limited. This contribution is strongly improved when the MD2 film, with the same thickness, is deposited trough a grid, the discontinuity of this layer inducing a significant decrease of the series resistance thanks to direct contact between AlPcCl and C_{60}. However, the participation of MD2 in the signal remains important, even if it decreases compared to the previous signal. It shows clearly that, even when it is discontinuous, the MD2 layer contributes to Jsc, which justifies that this type of OPV configuration exhibits the highest efficiency among the different OPV studied presently. The absorption curves of the structures ITO/MoO_3/CuI/AlPcCl/MD2 show that if the contribution to the absorption spectrum of MD2 deposited through a grid is smaller than that of a continuous film it is still clearly visible (Supporting Information S7)

In Table 1, we can see that, after optimisation of the MD2 layer thickness and morphology, by comparison with binary OPVs, the ternary AlPcCl/MD2/C_{60} OPV improves Jsc while FF decreases. In the case of continuous MD2 films, small FF and Jsc, may be related to the small electron mobility of MD2. Moreover, this limited carrier mobility singularly limits the thickness of the intercalated layer.

Therefore, the deposition of MD2 through a grid allows over-passing the bottleneck induced by the limited carrier mobility of MD2. If the idea of using structured organic layer, forming interpenetrated fingerlike junction to improve exciton dissociation is not new [43, 44], the

structured layer used in the present work is quite different. As a matter of fact, while usually, the idea was increasing the ED/EA interface area using nanostructured layers, in the present work the patterning consists in the formation of parallel micro-OPVs, using grid of microdimensions. It results that the interface area increase is not as large as in the case of nanopatterning, but with our micropatterning there is no difficulty for filling hollow areas not containing MD2. It is known that the use of nanowire arrays induces a low Voc due to the fact that dark current rapidly increases due to the direct contact of nanowires with the cathode due to high roughness of these structures [45]. Due to the micro size of our patterning such affect are nearly absent in our OPVs, even if there is a small increase of the dark current (S6), while Voc is only faintly affected.

As a matter of fact, about AlPcCl we have already shown [41] that the OPV performance depends significantly of the deposition rate of AlPcCl. Due to better crystallinity, films deposited at low deposition rate, 0.02-0.04 nm/s**,** give the best OPVs (Table 1). Nevertheless, it must be noted that larger Voc (# 0.8 V) are achieved for higher deposition rate. This is due to the fact that if a better crystallinity increases the short circuit current and therefore the OPV efficiency, it increases also the film roughness, which induces some leakage current and a limitation of the Voc value [41]. This fact can explain the Voc values obtained with the ternary OPVs. In the case of ternary OPCs, the MD2 layer intercalated between the AlPcCl and C_{60} layers increases the series resistance, which must decrease the leakage current of the OPV and therefore increase its Voc value. This explains the large Voc value of the ternary OPVs. The largest Voc values are obtained when the MD2 layer is continuous. When the MD2 layer is deposited through the grid, it is discontinuous, its resistance decreases and the Voc value also.

4. Conclusion

In the present work, we demonstrate that, the bottleneck due to a limited carrier mobility of the intercalated organic layer can be over passed using a clever geometrical approach. As a matter of fact, by depositing the intercalated layer through a grid, we decrease significantly the series resistance of the ternary OPC, while preserving most of its light absorption, which leads to an increase of Jsc. Thus, the Jsc value of the patterned ternary structure is increased by almost 60% compared to that of the structure with a continuous layer of the same thickness. That allows obtaining an efficiency of 4.19%, which is the highest efficiency obtained among all possible configurations of this family of binary and ternary OPVs.

References

1- Z. Hu, L. Ying, F. Huang, Y. Cao, Towards a bright future: polymer solar cells with power conversion efficiencies over 10%, SCIENCE CHINA Chemistry, 60 (2017) 571-582.

2- Guangye Zhang, Jingbo Zhao, Philip C. Y. Chow, Kui Jiang, Jianquan Zhang, Zonglong Zhu, Jie Zhang, Fei Huang, and He Yan, Nonfullerene Acceptor Molecules for Bulk Heterojunction Organic Solar Cells, Chem. Rev. 118 (2018) 3447−3507.

3- Baobing Fan, Difei Zhang, Meijing Li, Wenkai Zhong, Zhaomiyi Zeng, Lei Ying, Fei Huang & Yong Cao, Achieving over 16% efficiency for single-junction organic solar cells, Sci. China Chem. (2019) doi.org/10.1007/.s11426-01.9-9457-5

4- A. Leliège, J. Grolleau, M. Allain, P. Blanchard, D. Demeter, T. Rousseau, J. Roncali, Small D-p-A systems with s-phenylene-bridged accepting units as active materials for organic photovoltaics, Chem. Eur. J., 19 (2013) 9948-9960.

5- F. H. Scholes, T. Ehlig, M. James, K. H. Lee, N. Duffy, A. D. Scully, T. B. Singh, K. N. Winzen berg, K. Kemppinen, S. E. Watkins, Intraphase microstructure-understanding the impact on organic solar cell performance, Adv. Funct. Mater., (2013) DOI: 10.1002/adm.201300726.

6- Z. El Jouad, L.Barkat, N.Stephant, L.Cattin, N.Hamzaoui, A.Khelil, M.Ghamnia, M. Addou, M.Morsli, S.Béchu, C.Cabanetos, M.Richard-Plouet, P.Blanchard, J.C. Bernède, Ca/Alq_3 hybrid cathode buffer layer for the optimization of organic solar cells based on a planar heterojunction, Journal of Physics and Chemistry of Solids 98 (2016) 128–135.

7- M. Makha, L. Cattin, Y. Lare, L. Barkat, M. Morsli, M. Addou, A. Khelil,J. C. Bernède, MoO_3/Ag/MoO_3 anode in organic photovoltaic cells: Influence of the presence of a CuI buffer layer between the anode and the electron donor, Appl. Phys. Lett. 101 (2012) 233307.

8- S. Galindo, M. Ahmadpour, L. G. Gerling, A. Marsal, C. Voz, R. Alcubilla, J. Puigdollers, Influence of the density of states on the open-circuit voltage in small-molecule solar cells, Organic Electronics, 15 (2014) 2553-2560.

9- Y-J. Chang, J-L. Hsu, Y-H. Li, S. Biring, T-H. Yeh, J-Y. Guo, S-W. Liu, Carbazole based small molecules for vacuum deposited organic photovoltaic devices with open-circuit voltage exceeding1 V, Organic Electronics 47 (2017) 162-173.

10- S-C. Chen, Q. Zheng, Z. Yin, D. Cai, Y. Ma, High performance thermal-treatment-free tandem polymer solar cells with high fill factors, Organic Electronics, 47 (2017) 79-84.

11- R. Meerheim, C. Körner, B. Oesen, K. Leo, 10.4% Efficient triple organic solar cells containing near infrared absorbers, Appl. Phys. Lett., 108 (2016) 103302.

12- X. Che, Y. Li, S. R. Forrest, High fabrication yield organic tandem photovoltaics combining vacuum and solution processed subcells with 15% efficiency, Nature Energy, (2018) doi.org/10.1038/s41560-18-0134-z
13- Q. An, F. Zhang, J. Zhang, W. Tang, Z. Deng, B. Hu, Versatile ternary organic solar cells: a critical review, Energy Environ. Sci., 9 (2016) 281-322.
14- Q. An, F. Zhang, Q. Sun, M. Zhang, J. Zhang, W. Tang, X. Yin, Z. Deng, Efficient organic ternary solar cells with the third component as energy acceptor, Nano energy, 26 (2016) 180-191.
15- V. Sharapov, Q. Wu, A. Neshchadin, D. Zhao, Z. Cai, W. Chen, L. Yu. High performance ternary organic solar cells due to favored interfacial connection by non-fullerene electron acceptor with cross like molecular geometry, J. Phys. Chem. C, 122 (2018) 11305-11311.
16- K. Zhu, D. Tang, K. Zhang, Z. Wang, L. Ding, Y. Liu, L. Yuan, J. Fan, B. Song, Y. Zhou, Y. Li, A two-dimension-conjugated small molecule for efficient ternary organic solar cells. Organic Electronics. 48 (2017) 179-187.
17- L. Lu, W. Chen, T. Xu, L. Yu, High-performance ternary blend polymer solar cells involving both energy transfer ad hole relay processes. Nature Communications. (2015) DOI: 10.1038/ncomms8327.
18- W. Liu, H. Shi, W. Fu, L. Zuo, L. Wang, Chen H., Efficient ternary blend polymer solar cells with a bipolar diketopyrrolopyrrole small molecule as cascade material. Organic Electronics. 25 (2015) 219-224.
19- X. Ma, W. Gao, J. Yu, Q. An, M. Zhang, Z. Hu, J. Wang, W. Tang, C. Yang, F. Zhang, Ternary nonfullerene polymer solar cells with efficiency > 13.7% by integrating the advantages of the materials and two binary cells, Energy & Environmental Science, (2018) DOI: 10.1039/c8ee01107a
20- S. Sista, Y. Yao, Y. Yang, M. L. Tang, Z. Bao, Enhancement in open circuit voltage through a cascade-type energy band structure, Appl. Phys. Lett. 91 (2007) 223508.
21- T. D. Heidel, D. Hochbaum, J. M. Sussman, V. Songh, M. E. Bahlke, I. Hiromi, J. Lee, M. A. Baldo, Reducing recombination losses in planar organic photovoltaic cells using multiple step charge separation, J. App. Phys. 109 (2011) 104502.
22- C. W. Schlenker, V. S. Barlier, S. W. Chin, M. T. Whited, R. E. McAnally, S. R. Forrest, M. E. Thompson, Cascade organic solar cells, Chem. Mater., 23 (2011) 4132-4140.
23- K. Cnops, B. P. Rand, D. Cheyns, P. Heremans, Enhanced photocurrent and open-circuit voltage in a 3-layer cascade organic solar cell. Appl. Phys. Lett. 101 (2012) 143301.

24- B. Vereet, K. Cnops, D. Cheyns, P. Heremans, A. Stesmans, G. Zango, C. G. Claessens, T. Torres, B. P. Rand, Decreased recombination through the use of a non-fullerene acceptor in a 6.4 % efficient organic planar heterojunction solar cell, Adv. Energy Mater. 4 (2014) 1301413.
25- K. Cnops, B. P. Rand, D. Cheyns, B. Verreet, M. A. Empl, P. Heremans, 8.4% efficient fullerene-free organic solar cells exploiting long-range exciton energy transfer. Nature Communications. (2014) | 5:3406 | DOI: 10.1038/ncomms4406.
26- A. Barito, M. E. Sykes, B. Huang, D. Bilby, B. Frieberg, J. Kim, P. F. Green, M. Shtein, Universal Design Principles for Cascade Heterojunction Solar Cells with High Fill Factors and Internal Quantum Efficiencies Approaching 100%, Adv. Energy Mater. 4 (2014) 1400216.
27- M. A. Stevens, A. C. Arango, Open-Cirduit voltage exceeding the outmost HOMO-LUMO offset in cascade organic solar cells, Organic Electronics 37 (2016) 80-84.
28- YH. L. Lin, M. Koch, A. N. Brigeman, D. M. E. Freeman, L. Zhao, H. Bronstein, N. C. Giebink, G. D. Scholes, B. P. Rand, Enhanced sub-bandgap efficiency of a solid-state organic intermediate band solr cell using triplet-triplet annihilation, Energy & Environmental Science 10 (2017) 1465-1475.
29- C. Cabanetos, P. Blanchard, J. Roncali, Arylamine based photoactive push-pull molecular systems: a brief overview of the chemistry “made in Angers”, Chem. Rec. 19 (2019) 1-9.
30- A. Leliège, C-H. Le Régent, M. Allain, P. Blanchard, J. Roncali, Chem. Commun. 2012, 48, 8907].
31- J. Grolleau, F. Gohier, M. Allain, S. Legoupy, C. Cabanetos, P. Frère, Org. Electron. 42 (2017) 322-328.
32- J. W. Choi, C-H. Kim, J. Pison, A. Oyedele, D. tondelier, A. Leliège, E. Kirchner, P. Blanchard, J. Roncali, B. Geffroy, RSC Adv. 4 (2014) 5236-5242.
33- Z. El Jouad, M. Morsli, G. Louarn, L. Cattin, M. Addou, J.C. Bernède, Improving the efficiency of subphthalocyanine based planar organic solar cells through the use of MoO3/CuI double anode buffer layer, Solar Energy Materials & Solar Cells 141 (2015) 429-435.
34- J. C. Bernède, L. Cattin , M. Makha, V. Jeux, P. Leriche, J. Roncali, V. Froger, M. Morsli, M. Addou, Solar Energy Materials & Solar Cells 110 (2013) 107-114.
35- J.C. Bernède, L. Cattin, P. Predeep, XPS Study of the Band Alignment at the Interface ITO/CuI Technology Letters Vol.1, No.1 (2014) 2-10.
36- P. Peumans, A. Yakimov, S. R. Forrest, Small molecular weight organic thin-film photoconductors and solar cells, J. Appl. Phys. 93 (2003) 3693-3723.

37- P. Peumans, V. Bulovic, S.R. Forrest, Efficient photon harvesting at high optical intensities in ultrathin organic double-heterostructure photovoltaic diodes, Appl. Phys. Lett. 76 (2000) 2650–2652.
38- B.P. Rand, J. Li, J. Xue, R.J. Holmes, M.E. Thompson, S.R. Forrest, Organic Double-Heterostructure Photovoltaic Cells Employing Thick Tris(acetylacetonat)ruthenium(III) Exciton-Blocking Layers, Adv. Mater. 17 (2005) 2714–2718.
39- B. Ebenhoch, N. B. A. Prasetya, V. M. Rotello, G. Cooke, Solution-processed boron subphthalocyanine derivatives as acceptors for organic bulk-heterojunction solar cells. J. Mater. Chem. A. 3 (2015) 7345-7352.
40- N. Beaumont, S. W. Cho, P. Sullivan, D. Newby, K. E. Smith and T. S. Jones, Boron Subphthalocyanine Chloride as an Electron Acceptor for High‐Voltage Fullerene‐Free Organic Photovoltaics Adv. Funct. Mater. 22 (2012) 561).
41- A. Mohammed-Krarroubi, M. Morsli, A. Khelil, L. Cattin, L. Barkat, S. Tuo, Z. El Jouad, G. Louarn, M. Ghamnia, M. Addou, J. C. Bernède, The influence of deposition rates on properties of AlPcCl thin films and on the performance of planar organic solar cells. Physica Status Solidi, (2017) 1700364.
42 - L. Cattin, Z. El Jouad, M. B. Siad, A. Mohammed Krarroubi, G. Neculqueo, L. Arzel, N. Stephant, M. Talamo, F. Martinez, M. Addou, A. Khelil, M. Morsli, P. Blanchard, and J. C. Bernède, Highlighting the possibility of parallel mechanism in planar ternary photovoltaic cells, AIP Advances 8 (2018) 115329 (2018); doi: 10.1063/1.5037531.
43- Shuwen Yu, Carola Klimm, Peter Schäfer, Jürgen P. Rabe, B. Rech, Norbert Koch, Organic photovoltaic cells with interdigitated structures based on pentacene nanocolumn arrays, Organic Electronics 12 (2011) 2180-2184.
43- D. M. Nanditha, M. Dissanayake, A. A. D. T. Adikaari, R. J. Curry, R. A. Hatton, S. R. P. Silva, Nnoimprinted large area heterojunction pentacene-C60 photovoltaic device, Apll. Phys. Let. 90 (2007) 253502.
44- Jie Zhang , Philippe Barboux , and Thierry Pauporté. Electrochemical Design of Nanostructured ZnO Charge Carrier Layers for Efficient Solid-State Perovskite-Sensitized Solar Cells, Adv. Energy Mater. 4 (2014) 1400932.

Figures

Figure 1: Chemical structures of the investigated organic materials.

Figure 2: Band scheme of the ternary structure PHJ-OPV AlPcCl/MD2/C_{60}

Figure 3: J-V characteristics of (a) the different binary OPVs and (b) different typical ternary AlPcCl/MD2/C_{60} OPV, the MD2 layer thickness and morphology being used as parameters.

Figure 4: Visualization of the grid and of the corresponding deposited film.

Figure 5: Surface profile of a MD2 film deposited through a grid obtained with a profilometer.

Figure 6: Schematization of the geometrical section of a ternary PHJ-OPV with a MD2 layer deposited through a grid and corresponding band schemes.

Figure 7: (a) -EQE spectra of ternary PHJ-OPV with different MD2 layer thickness and configurations, (■) MD2 9 nm thick deposited through a grid, (▼) Continuous MD2 layer thick of 9 nm, (●)Continuous MD2 layer thick of 15 nm.

(b) – Light absorption of the different layers [MD2 (thin line), AlPcCl (□•□•□) and C60 (□□□)] and when they are stacked (thick line).

Table

Table 1: Parameter of the cells of the different OPC categories.

AlPcCl

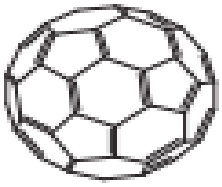

C60

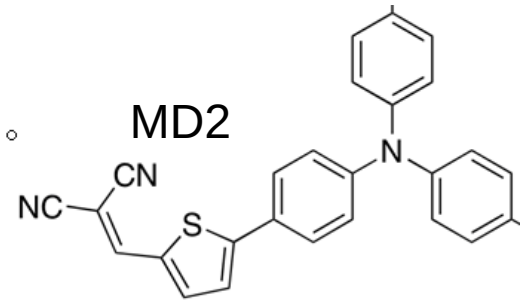

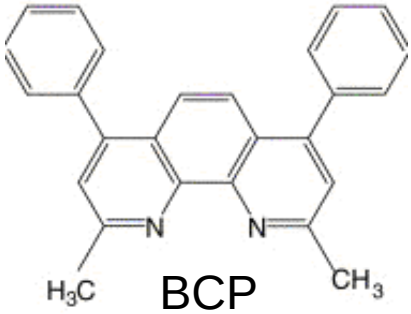

Figure 1.

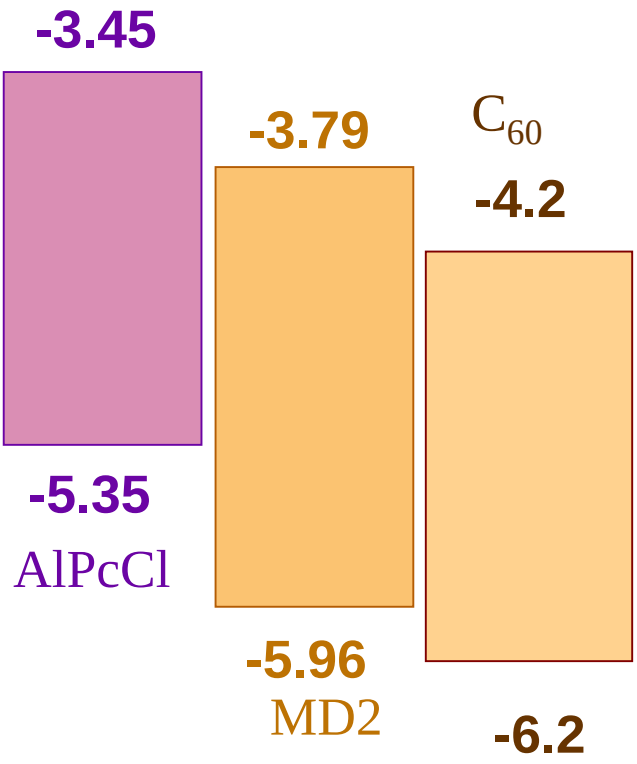

Figure 2.

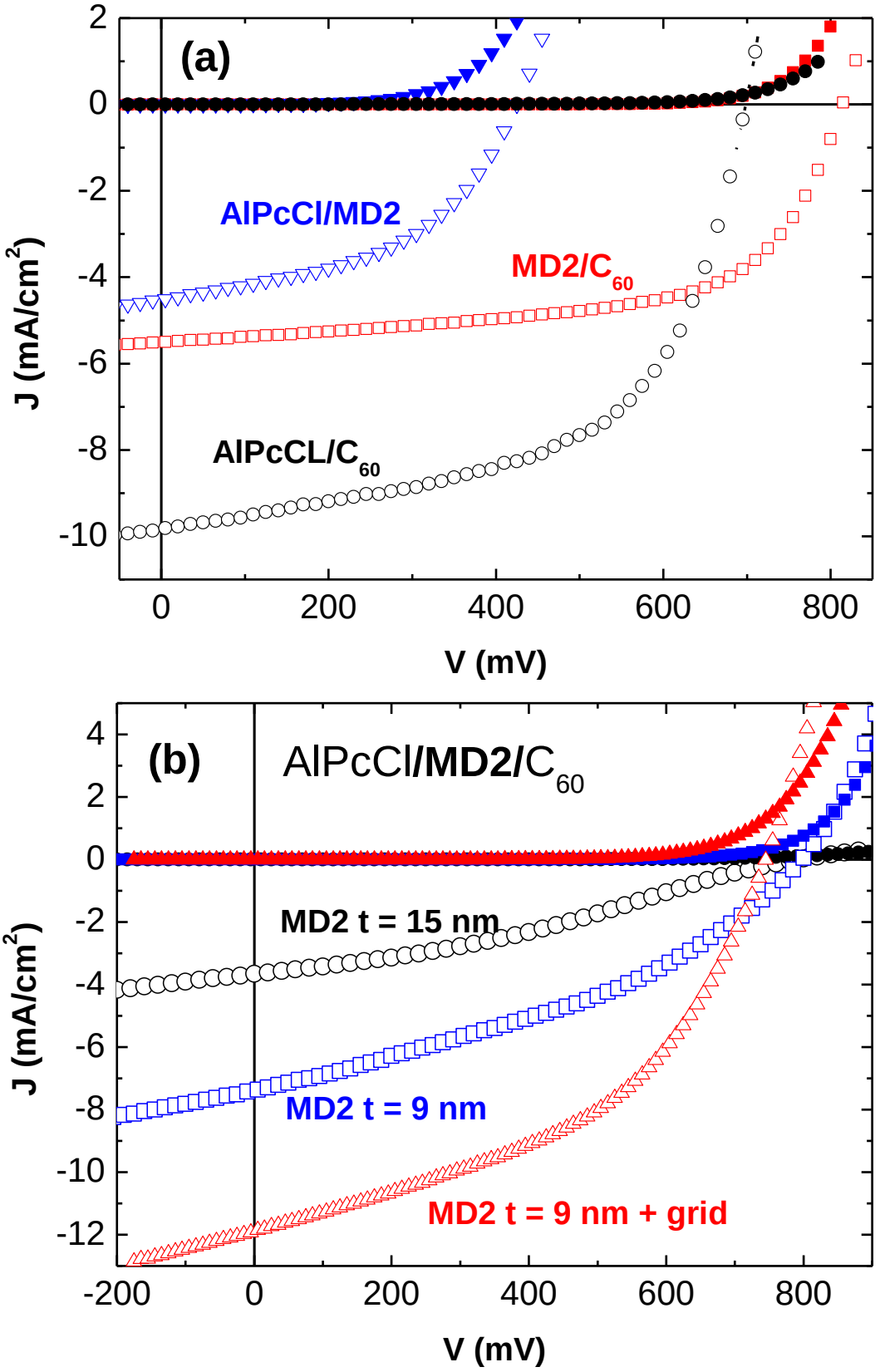
(a)
AlPcCl/MD2
MD2/C60
AlPcCL/C60
J (mA/cm2)
V (mV)
(b)
AlPcCl/MD2/C60
MD2 t = 15 nm
MD2 t = 9 nm
MD2 t = 9 nm + grid
J (mA/cm2)
V (mV)

Figure 3.

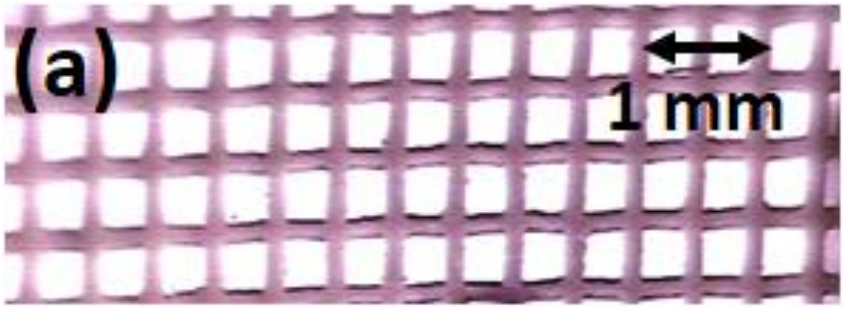

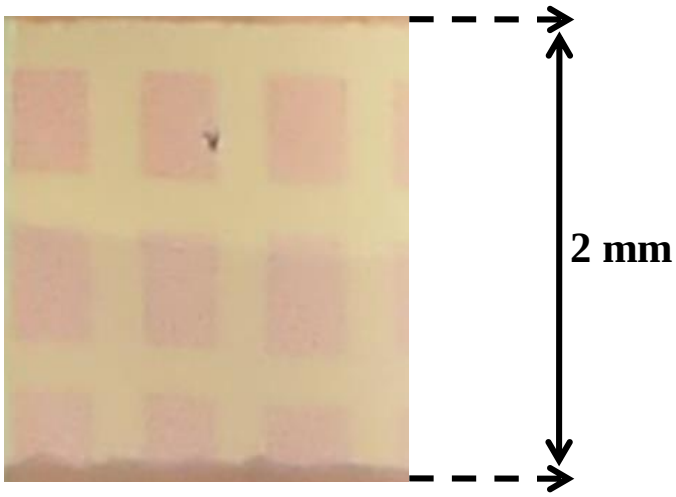

Figure 4

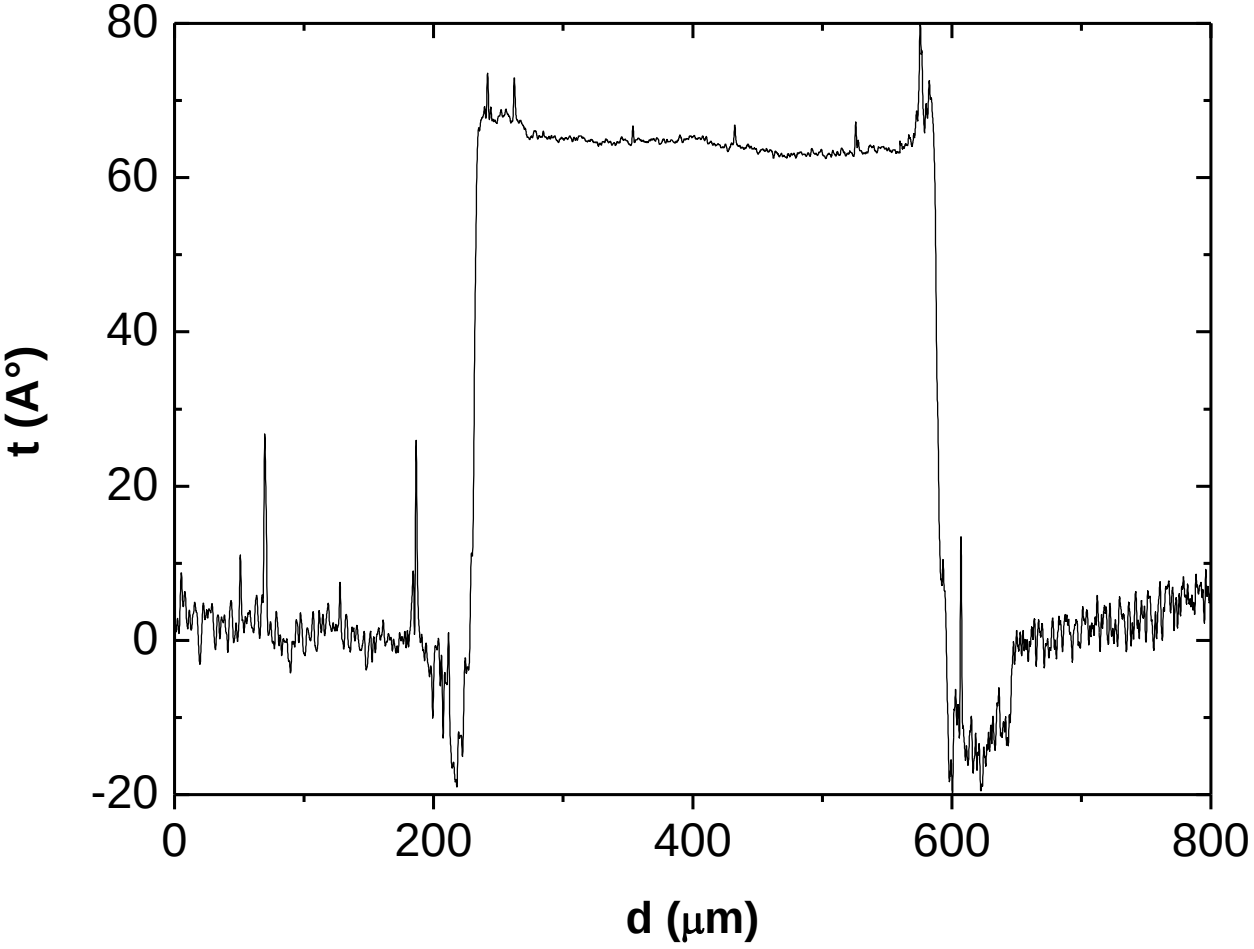

Figure 5.

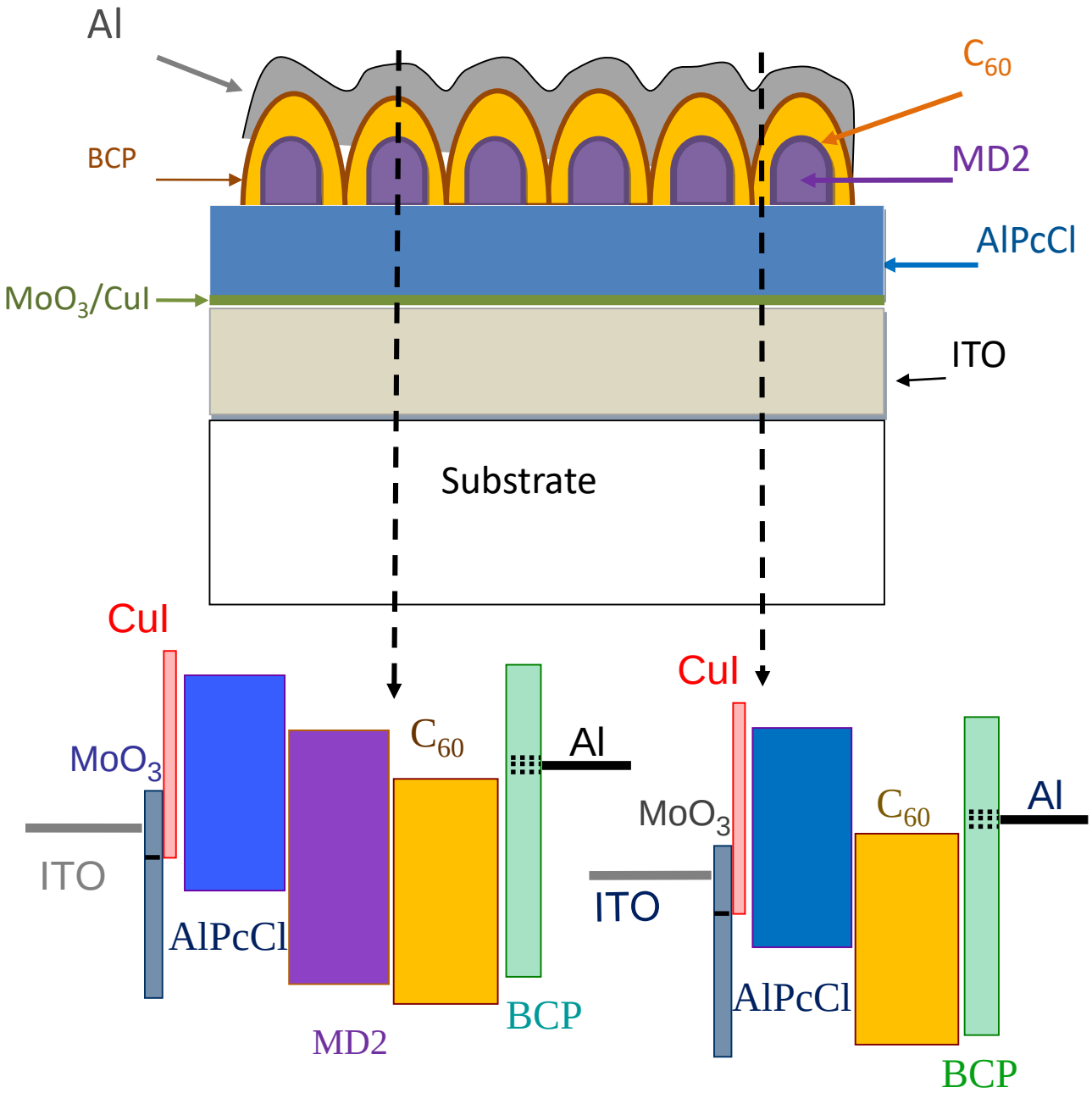
Al
BCP
C_{60}
MD2
AlPcCl
MoO_3/CuI
ITO
Substrate
CuI
MoO_3
ITO
AlPcCl
MD2
C_{60}
Al
BCP
CuI
MoO_3
ITO
AlPcCl
C_{60}
Al
BCP

Figure 6

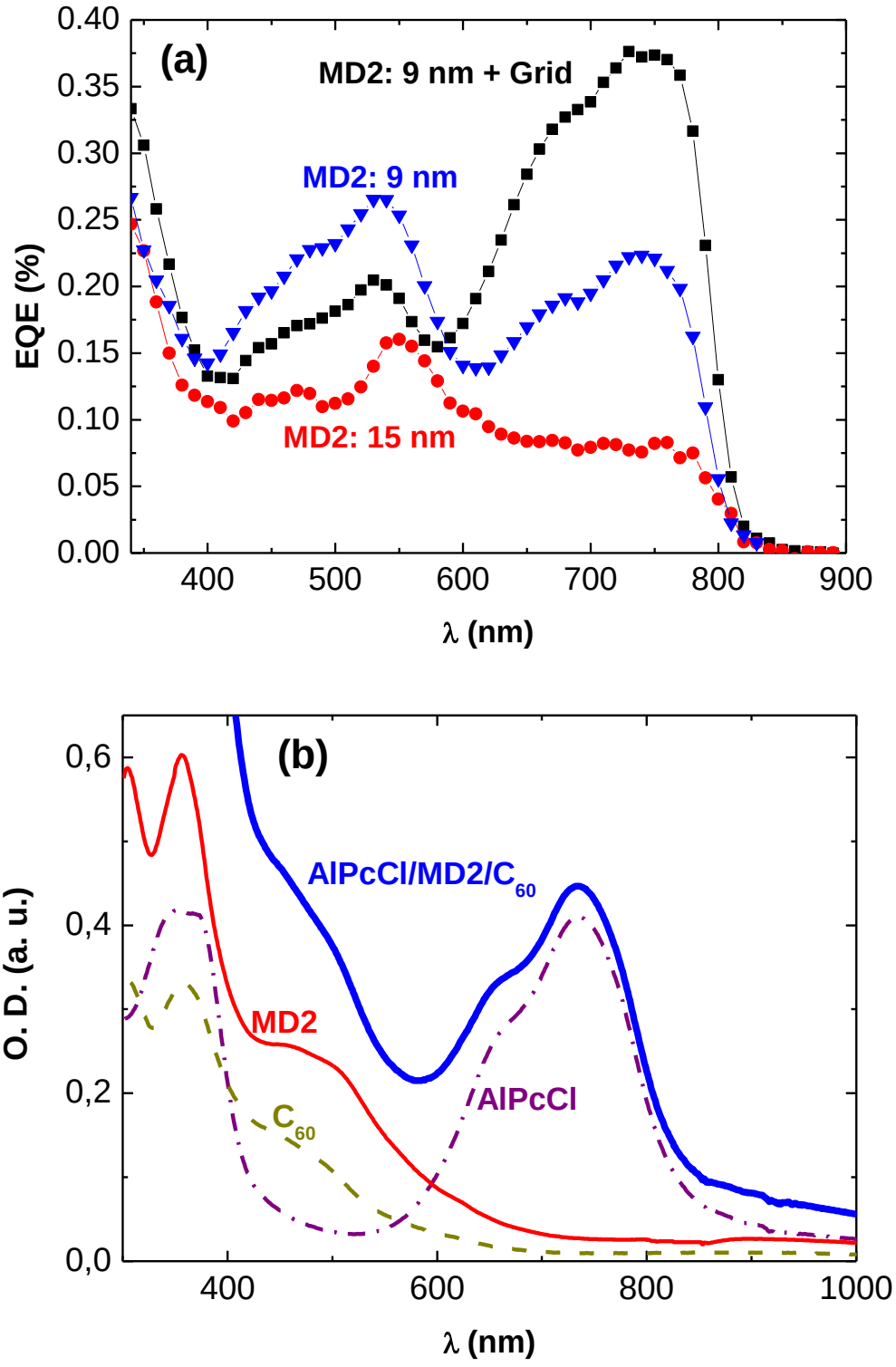
(a)
MD2: 9 nm + Grid
MD2: 9 nm
MD2: 15 nm
EQE (%)
λ (nm)
0.40
0.35
0.30
0.25
0.20
0.15
0.10
0.05
0.00
400
500
600
700
800
900
(b)
AlPcCl/MD2/C60
MD2
AlPcCl
C60
O. D. (a. u.)
λ (nm)
0,6
0,4
0,2
0,0
400
600
800
1000

Figure 7.

AlPcCl/MD2/C_{60} ternary OPVC and corresponding binary cells						
Sample (thickness, nm)	Voc (V)	Jsc (mA/cm^2)	FF (%)	η (%)	Rs (Ω)	Rsh (Ω)
MD2 (15)/C_{60}	0.81	5.49	59	2.75	12	500
AlPcCl (26)/ C_{60} (40)	0.70	9.61	59.5	3.97	10	450
AlPcCl (20)/ MD2 (7)	0.42	4.50	48	1.00	11	300
AlPcCl (20)/ MD2 (15)/C_{60} (40)	0.80	3.66	30	0.93	400	800
AlPcCl (20)/ MD2 (9)/C_{60} (40)	0.80	7.37	38	2.24	28	250
AlPcCl (20)/ MD2 (9)/C_{60} (40) (MD2 through grid)	0.75	11.90	47	4.19	9	200

Table 1: Parameter of the cells of the different OPC categories.

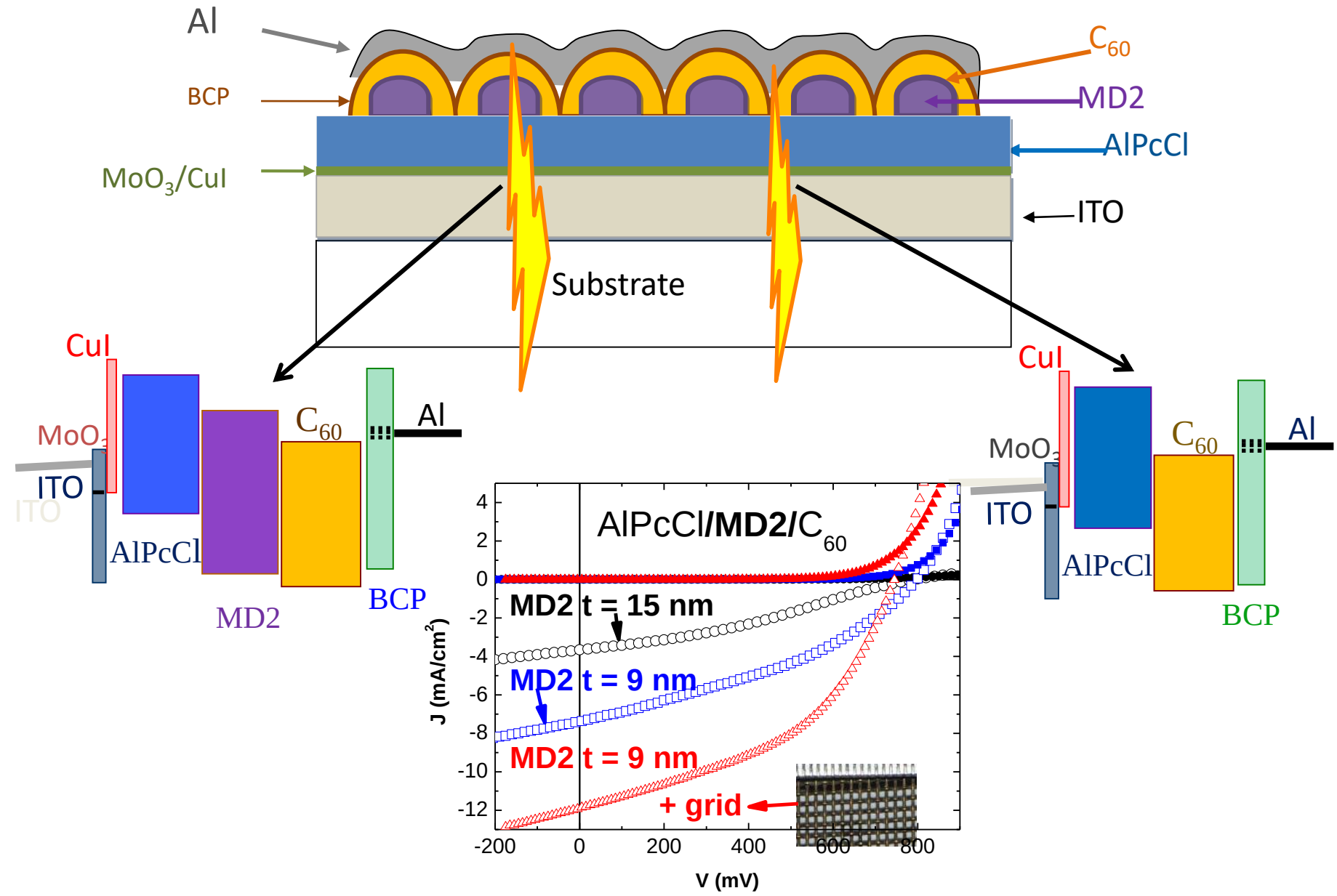
Al
BCP
MoO_3/CuI
C_{60}
MD2
AlPcCl
ITO
Substrate
CuI
MoO_3
ITO
AlPcCl
MD2
C_{60}
BCP
Al
AlPcCl/MD2/C_{60}
MD2 t = 15 nm
MD2 t = 9 nm
MD2 t = 9 nm
+ grid
J (mA/cm^2)
V (mV)
4
2
0
-2
-4
-6
-8
-10
-12
-200
0
200
400
600
800